THE ASTROPHYSICAL JOURNAL, 336:429–441, 1989 January 1

NARROW ULTRAVIOLET EMISSION LINES FROM SN 1987A: EVIDENCE FOR CNO PROCESSING IN THE PROGENITOR

C. FRANSSON,[1] A. CASSATELLA,[2,3] R. GILMOZZI,[2,3] R. P. KIRSHNER,[4] N. PANAGIA,[5] G. SONNEBORN,[6] AND W. WAMSTEKER[2]

Received 1988 February 24; accepted 1988 June 23

ABSTRACT

UV observations of SN 1987A with the *IUE* satellite are reported. Spectra after 1987 May 24 show emission lines of He II, C III, N III, N IV, N V, and O III, increasing in strength with time. High-resolution observations show that the widths of the lines are less than ~ 30 km s^{-1} (FWHM). The line strengths and widths indicate an origin in a photoionized low-density circumstellar gas, lost by the progenitor in its red supergiant phase. The most likely excitation source is the EUV burst at the time of the shock breakout. The time evolution is consistent with that expected from a fluorescent light echo by a circumstellar shell. A nebular analysis reveals a large nitrogen overabundance with $N/C = 7.8 \pm 4$ and $N/O = 1.6 \pm 0.8$. These are respectively factors of 37 and 12 higher than the solar values, implying that the gas has undergone substantial CNO processing. To reveal CNO-processed material at the surface, the progenitor of SN 1987A is likely to have lost much of its hydrogen envelope before the explosion. This, and the existence of the shell, are consistent with models where a red supergiant evolves to the blue supergiant stage before exploding.

Subject headings: nucleosynthesis — stars: abundances — stars: circumstellar shells — stars: individual (SN 1987A) — stars: supernovae — ultraviolet: spectra

I. INTRODUCTION

The initial *International Ultraviolet Explorer* (*IUE*) observations of SN 1987A after the discovery on 1987 February 24 showed a strong UV continuum with a color temperature of $\sim 14{,}000$ K (Cassatella *et al.* 1987; Kirshner *et al.* 1987*a*). The UV flux, however, rapidly decreased, and after a few weeks the spectrum was instead characterized by a strong UV deficit. This is most easily interpreted as a result of blanketing by a large number of wide resonance lines (velocities $\sim 25{,}000$ km s^{-1}) from the expanding envelope of the supernova (Fransson *et al.* 1987; Lucy 1987). As a result of this scattering, photons created in the far-UV perform a random walk in space and are redshifted in each scattering. Thus most far-UV photons emerge longward of ~ 2700 Å. In mid-March only the emission from the two additional stars in the *IUE* aperture could thus be seen shortward of ~ 1800 Å (Gilmozzi *et al.* 1987; Sonneborn, Altner, and Kirshner 1987). After ~ 100 days, observations, however, revealed a number of *narrow* emission lines of highly ionized gas (Wamsteker *et al.* 1987*b*). Subsequent observations confirmed the presence of these lines and a further increase in their fluxes (Kirshner *et al.* 1987*b*). Because of the time variation it was immediately clear that they originated in the supernova neighborhood. In this paper we discuss observations through 1988 April, and their implications for the properties of the UV-emitting gas, including the origin of the emission lines and their excitation. Preliminary reports have been given by Cassatella (1987) and Kirshner (1988). We start with a discussion of the observations in § II, and in § III we use a nebular analysis to derive the physical conditions in the emission region. In § IV we discuss the origin of the emission lines, and finally in § V we explore the implications for the evolution of Sanduleak $-69°$ 202.

II. OBSERVATIONS

Since the discovery on 1987 February 24, SN 1987A has been vigorously monitored by *IUE* (e.g., Wamsteker *et al.* 1987*a*; Panagia *et al.* 1987*b*; Kirshner *et al.* 1987*b*). In Table 1 we give the observing log in the short-wavelength range of the *IUE* satellite, 1150–1950 Å, from 1987 May until 1988 April. Observations from both VILSPA and the Goddard Space Flight Center (GSFC) are included. Because of the faintness of the emission in the short-wavelength band, all observations except one, discussed below, have been made in the low-resolution mode. In the short-wavelength range the emission from the supernova fell very rapidly, by a factor of $\sim 10^3$, during the first few days, and in mid-March essentially all of the emission was due to the two additional stars in the *IUE* aperture. These stars are early B stars close to the main sequence (Gilmozzi *et al.* 1987; Sonneborn, Altner, and Kirshner 1987). The separations from SN 1987A are 2.″9 and 1.″6, respectively (Walborn *et al.* 1987). Since this is close to the spatial resolution of *IUE*, they contribute an ultraviolet background against which all measurements have to be performed.

In Figure 1 we show a sample of the observed spectra on 1987 May 24, June 24, July 26, September 20, and November 13, and 1988 February 13 and April 14. All spectra have been corrected for a total reddening of $E(B-V) = 0.2$, of which 0.05 originates from the Galactic foreground and 0.15 from the LMC (Panagia *et al.* 1987*a*). We have used the extinction laws of Savage and Mathis (1979) for the Galaxy, and the 30 Doradus law by Fitzpatrick (1986) for the LMC. The same figure also shows the spectrum of the supernova field from an average of five spectra taken between 1987 March 13 and 28,

[1] Stockholm Observatory.
[2] *IUE* Observatory, European Space Agency. Affiliated with the Astrophysics Division, Space Sciences Department, ESA.
[3] On leave from Istituto Astrofisica Spaziale, CNR, Frascati, Italy.
[4] Space Telescope Science Institute and University of Catania.
[5] Harvard-Smithsonian Center for Astrophysics. Affiliated with the Astrophysics Division, Space Sciences Department, ESA.
[6] Astronomy Programs, Computer Sciences Corporation. Staff member of the *IUE* Observatory, at the Laboratory for Astronomy and Solar Physics, NASA/Goddard Space Flight Center.

TABLE 1

OBSERVING LOG OF SN 1987A FROM 1180 TO 1950 Å (1987 May 1–1988 May 1)[a]

SWP IMAGE Number	Date (UT)	Duration (minutes)	Station
30512	1987 Mar 13	240	GSFC
30522	1987 Mar 14	181	VILSPA
30547	1987 Mar 16	240	GSFC
30592	1987 Mar 22	300	GSFC
30637	1987 Mar 28	185	VILSPA
30907	1987 May 4	230	GSFC
30929	1987 May 7	60	GSFC
30974	1987 May 14	120	GSFC
31000	1987 May 19	180	GSFC
31040	1987 May 24	195	VILSPA
31064	1987 May 30	180	GSFC
31125	1987 Jun 9	200	VILSPA
31132	1987 Jun 11	195	VILSPA
31154	1987 Jun 14	180	VILSPA
31166	1987 Jun 16	180	GSFC
31177	1987 Jun 17	128	VILSPA
31245	1987 Jun 24	260	VILSPA
31273	1987 Jul 1	240	GSFC
31274	1987 Jul 1	140	GSFC
31319	1987 Jul 10	240	VILSPA
31320	1987 Jul 11	120	VILSPA
31334	1987 Jul 12	80	GSFC
31371	1987 Jul 20	240	GSFC
31372	1987 Jul 20	105	GSFC
31420	1987 Jul 26	240	VILSPA
31421	1987 Jul 26	120	GSFC
31462	1987 Aug 3	240	GSFC
31463	1987 Aug 3	85	GSFC
31534	1987 Aug 10	220	VILSPA
31592	1987 Aug 19	240	GSFC
31651	1987 Aug 27	210	GSFC
31676	1987 Aug 30	240	GSFC
31818	1987 Sep 10	90	GSFC
31819	1987 Sep 10	240	GSFC
31892	1987 Sep 20	150	GSFC
31893	1987 Sep 20	200	VILSPA
32030	1987 Oct 8	240	GSFC
32031	1987 Oct 9	90	GSFC
32168	1987 Oct 26	155	VILSPA
32314	1987 Nov 13	235	VILSPA
32395	1987 Nov 26	90	GSFC
32404	1987 Nov 26	240	GSFC
32532	1987 Dec 16	240	VISLPA
32619	1987 Dec 25	240	GSFC
32620	1987 Dec 25	80	GSFC
32717	1988 Jan 13	190	VILSPA
32797	1988 Jan 27	240	GSFC
32798	1988 Jan 27	70	GSFC
32910	1988 Feb 13	70	VILSPA
32911	1988 Feb 13	212	VILSPA
32938	1988 Feb 18	180	VILSPA
32984	1988 Feb 25	60	GSFC
32985	1988 Feb 25	60	GSFC
33104	1988 Mar 17	70	VILSPA
33105	1988 Mar 17	240	VILSPA
33279	1988 Apr 14	60	VILSPA
33280	1988 Apr 14	200	VILSPA

[a] Also included are the spectra from 1987 March used for deriving an average background spectrum.

which is mainly from the two background stars, Nos. 2 and 3. Spectra taken in April and the beginning of May are essentially the same, with little emission other than from these stars. At the end of May, however, a number of narrow emission lines appeared, which grew stronger with time. Based on the wavelengths of the emission lines, we identify these as N v λλ1238–1242, N iv] λλ1483–1486, He ii λ1640, O iii] λ1664, N iii] λλ1747–1754, and C iii] λλ1907–1909. Although N v λ1240 is the strongest line throughout the whole evolution, its measurement is rather difficult, expecially in the early spectra in May and June. The main reason for this is the highly nonuniform background from the two additional B stars in the aperture. To minimize the influence of these, we have therefore subtracted a "background" spectrum obtained as an average of five spectra in March (see Table 1 and Fig. 1). To illustrate this and to bring out the weaker features, we have added the well-exposed spectra obtained from this subtraction from the same periods of time. Since the time variation is rather smooth, this increases the signal-to-noise level considerably. In Figure 2 we show these averaged spectra from 1987 June, July, August, September, October–November, 1987 December–1988 February, and 1988 February–April. In addition to this constant background, emission from the supernova again started to leak out from the envelope below ~1450 Å and above ~1700 Å. From Figure 2 it is apparent that this "continuum" increased with time. As in the early spectra, some of the features may be superpositions of several absorption components from resonance lines in the supernova envelope. This complicates the analysis, especially of the C iii] region.

The subtraction procedure is useful in bringing out additional emission in the strong absorption regions of permitted lines, such as N v, Si iv, and C iv. These lines suffer both from absorption lines in the background stellar spectra and from interstellar absorption along the line of sight. While the N v line is very prominent, there is, however, no indication of emission in the Si iv and C iv regions at 1400 and 1550 Å, respectively. We note, however, that the early high-resolution spectra showed a number of strong *absorption* features in both these lines, likely to arise in coronal gas in our own Galaxy and in the LMC (de Boer *et al.* 1987; Dupree *et al.* 1987; Blades *et al.* 1988). In particular, the component at 282 km s^{-1} is close to the redshift, 284 ± 6 km s^{-1}, derived from the high-resolution observations (Panagia *et al.* 1987*b*). Most of the Si iv and C iv emission is thus likely to be absorbed, since the width of the absorption lines (75–100 km s^{-1}) exceeds that of the emission lines (~30 km s^{-1}). The nondetection of Si iv and C iv emission therefore does not imply that these lines are absent. The fact that the N v line clearly stands out indicates that the interstellar N v column density is small, in agreement with the early high-resolution observations (Fransson *et al.* 1987).

The reddening-corrected fluxes at the different dates are given in Table 2. To avoid saturation effects above ~1700 Å, both long and short exposures were combined for several dates. In all cases the fluxes have been measured from the local continuum level. We estimate that the errors in these measurements are ~25% for the strong N iii] line, but can reach ~40% for N v and C iii], especially in the early spectra. In Figure 3 we show the time evolution of the fluxes. As anticipated, the N v line shows a large scatter, as does O iii] λ1664. We ascribe the latter to the presence of the nearby Al ii λ1670 absorption. For future discussion it is of interest to compare the time evolution of lines from different ionization stages, in particular N iii] λ1750, N iv] λ1486, and N v λ1240. Whereas the N iii] and N v lines show a steady increase, the flux of the N iv] line is fairly constant. The larger scatter of the N iv] line compared with the N iii] line is due to the lower sensitivity of the SWP camera in the N iv] region. The C iii] line is initially weak and severely affected by the varying underlying continuum from the supernova, but shows a trend similar to the N

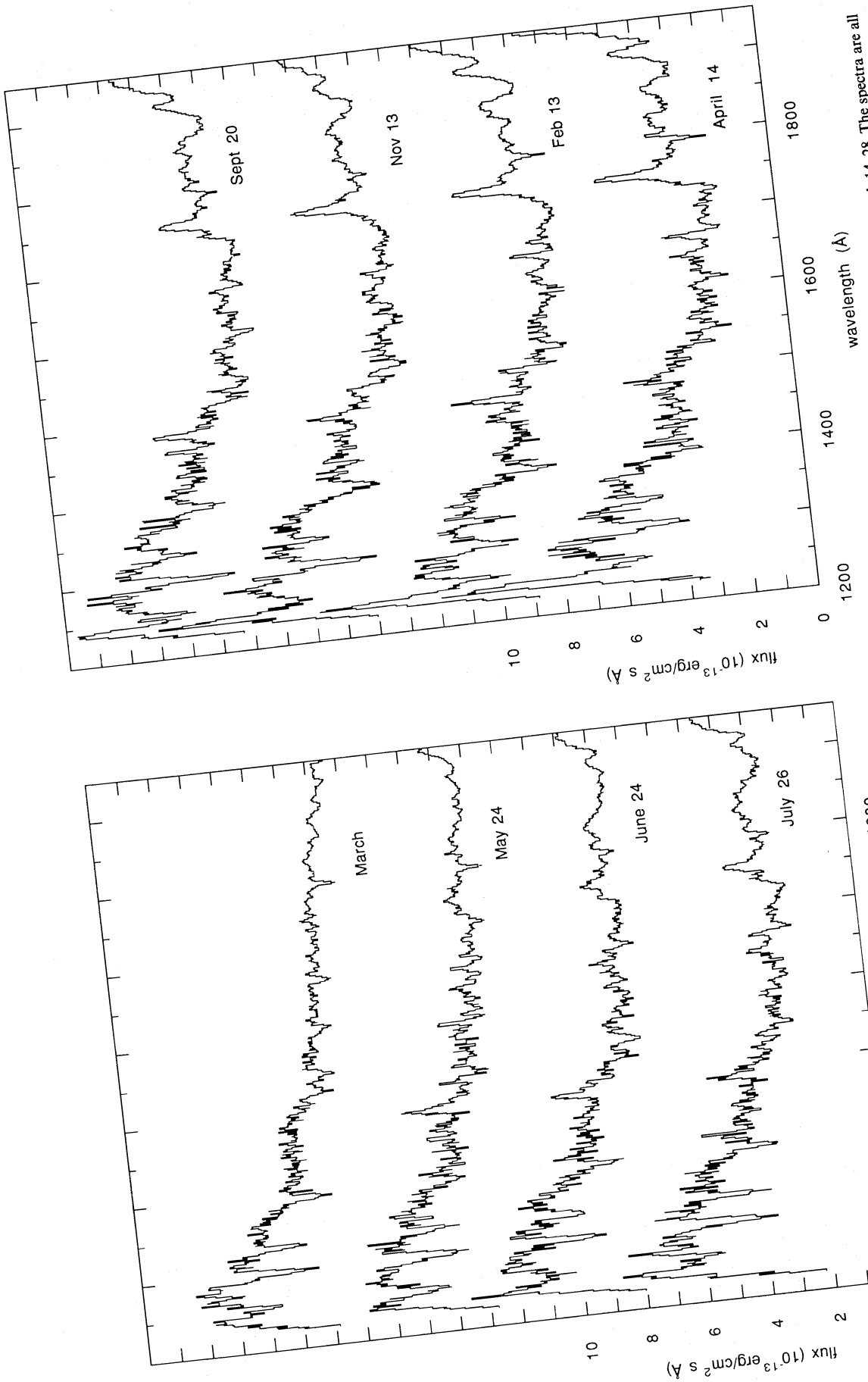

FIG. 1.—Evolution of the UV spectrum of SN 1987A from 1987 May to 1988 April. The first spectrum, from March, is an average "background" spectrum from 1987 March 14–28. The spectra are all reddening-corrected with $E(B-V) = 0.20$ (see text). Each spectrum is shifted by 5×10^{-13} ergs cm^{-2} s^{-1} Å^{-1}.

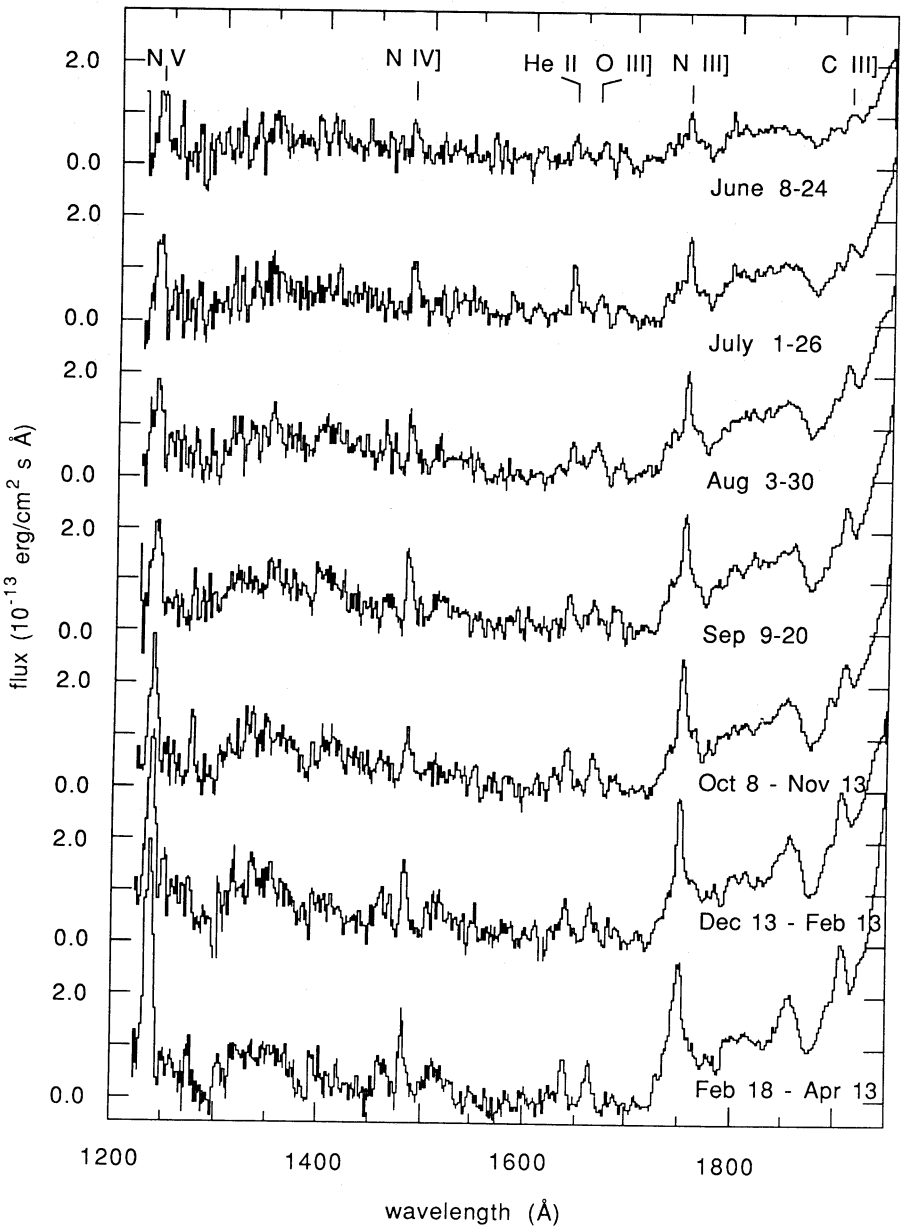

FIG. 2.—Averaged spectra obtained as the result of an average of the difference of the spectra from the periods indicated and the mean March spectrum. The positions of the strongest emission lines are shown. Note especially the steady increase in the N III] λ1750 line and the strong N V λ1240 line.

III] and N V lines. This may also be the case with the O III] line, but the scatter is large. The He II line seems fairly constant. Most of the short-term variations in the fluxes, especially of N V and N IV], can be ascribed to observational errors.

To discriminate between possible origins for the emission, the widths of the lines are important. In the spectra the mean width (FWHM) of the N IV] doublet is ~7.8 Å (or 4.7 Å after correction for the doublet separation), while the mean width of the He II line is ~5.5 Å. The resolution of the SWP camera is discussed by Cassatella, Barbero, and Benvenuti (1985). They find that the resolution near N IV] reaches a maximum of ~4.6 Å (FWHM), while it is ~5.4 Å near He II. Thus, we conclude from the low-dispersion observations that all the well-observed emission lines are unresolved, implying that the FWHM is less than ~900 km s^{-1}. There is no evidence for any systematic shifts of the peaks of any of the lines, within the resolution (~2 Å ~300 km s^{-1}).

Because of the increase in the line fluxes, a high-resolution observation with *IUE* could be performed with the SWP camera on 1987 November 25 (Panagia *et al.* 1987*b*). The spectrum, SWP 32394, was obtained during a double-shift observation with an exposure time of 450 minutes. A detailed discussion of these observations will be given in a subsequent paper (Cassatella *et al.* 1988). Here we discuss only the results relevant to this paper. In Figure 4 we show the region around 1910 Å. As can be seen, the C III] lines at 1906.68 and 1908.73 Å are both displaced by a velocity of 284 ± 6 km s^{-1}. In addition, the N III] 1749.67, 1752.16, and 1753.98 Å components are all seen at the same velocity (Panagia *et al.* 1987*b*). The fact that this coincides with the highest velocity component of most

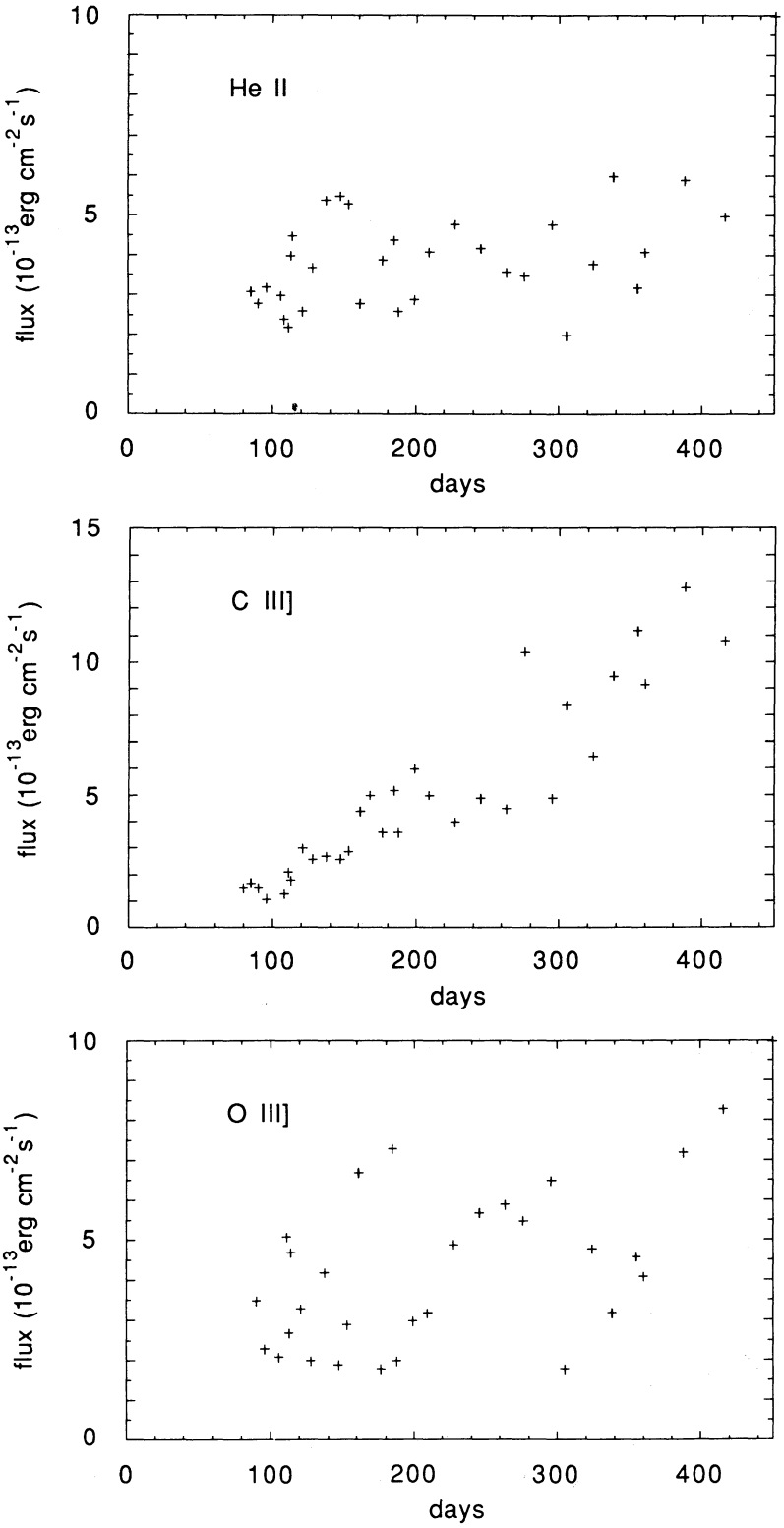

FIG. 3.—Time evolution of the flux of the emission lines. The flux is in 10^{-13} ergs cm^{-2} s^{-1}, and the time is measured in days since the explosion.

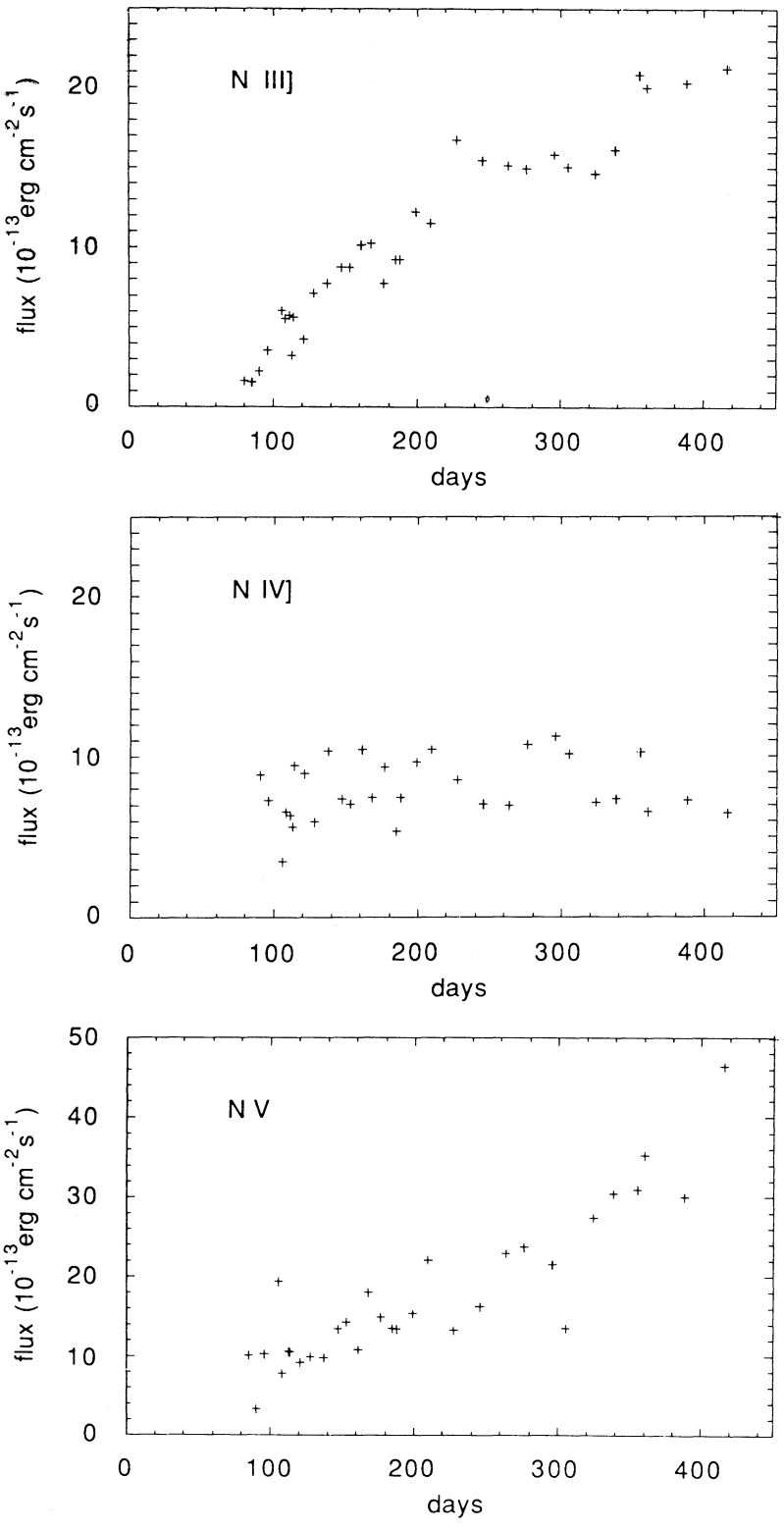

FIG. 3—*Continued*

TABLE 2

LINE FLUXES, REDDENING-CORRECTED WITH $E(B-V) = 0.2$.[a]

SWP	DATE	DAY AFTER EXPLOSION	LINE FLUXES (10^{-14} ergs cm^{-3} s^{-1})					
			N V	N IV]	He II	O III]	N III]	C III]
31000	1987 May 19	85	102	Noisy	31	...	16:	17:
31040	1987 May 24	90	34:	89	28	35:	23	15:
31064	1987 May 30	96	103	73:	32:	23:	36	11:
31125	1987 Jun 9	106	195:	35:	30	21::	61	...
31132	1987 Jun 11	108	79	66	24:	...	56	13::
31154	1987 Jun 14	111	Noisy	64	22:	51:	58	21
31166	1987 Jun 16	113	107	57	40	27:	33	18
31177	1987 Jun 17	114	106	95::	45	47	57	...
31245	1987 Jun 24	121	93	90	26	33:	43	30:
31273	1987 Jul 1	128	100	60	37:	20::	72	26:
31319	1987 Jul 10	137	99	104::	54	42	78	27:
31371–72	1987 Jul 20	147	135	74	55	19	88	26:
31420–21	1987 Jul 26	153	144:	71	53	29	88	29
31462–63	1987 Aug 3	161	109	105	28	67	102	44
31534	1987 Aug 10	168	181	75	...	...	103	50::
31592	1987 Aug 19	177	150	94	39	18:	78	36
31651	1987 Aug 27	185	136:	54	44	73	93	52
31676	1987 Aug 30	188	135	75	26	20	93	36
31818–19	1987 Sep 10	199	155	97	29:	30	123	60
31892–93	1987 Sep 20	209	222	105	41	32	116	50
32030–31	1987 Oct 8	227	133	86	48	49	168	40
32168	1987 Oct 26	245	163	71::	42	57	155	49
32314	1987 Nov 13	263	230	70	36:	59	152	45
32395–404	1987 Nov 26	276	238	108	35	55:	150	104:
32532	1987 Dec 16	296	216	113:	48	65	159	49
32619–20	1987 Dec 25	305	136::	102:	20::	18::	151	84
32717	1988 Jan 13	324	275:	72:	38:	48:	147	65:
32798	1988 Jan 27	338	305	74	60	32:	162	95
32910–11	1988 Feb 13	355	310	103	32	46:	209	112
32938	1988 Feb 18	360	353	66:	41	41	201	92
33104–05	1988 Mar 17	388	301	73	59	72	204	128
33279–80	1988 Apr 14	416	465	65	50	83	213	108

[a] See text.

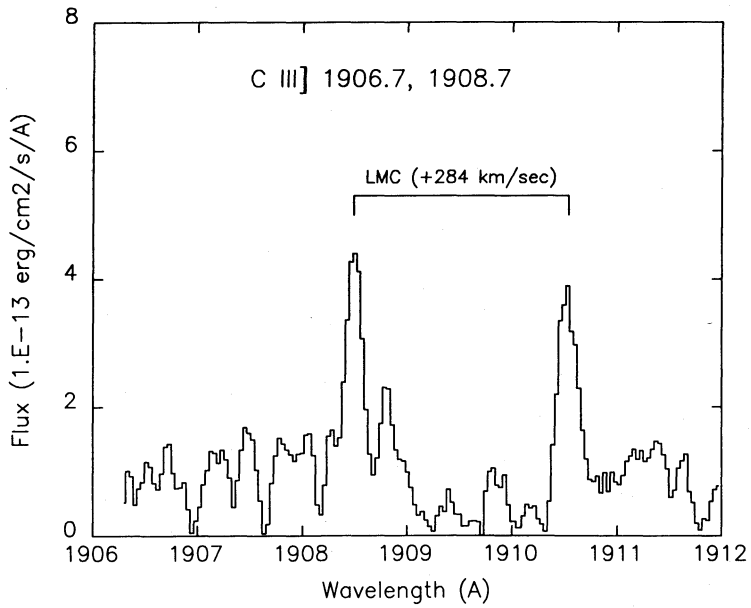

FIG. 4.—High-resolution spectrum from 1987 November 25 of the C III] region

absorption lines of interstellar origin (de Boer *et al.* 1987; Blades *et al.* 1988) raises the possibility that this absorption component can be associated with the supernova neighborhood. Also the Na I and Ca II lines possessed a strong absorption component at 284.8 km s^{-1} (Vidal-Madjar *et al.* 1987). Although the noise in our high-dispersion spectra is considerable, the fact that all lines show the same velocity displacement confirms the reality of the line features. In addition, He II λ1640.4 and the 1483.3 Å component of the N IV] line were also detected at the same velocity. Unfortunately, the 1486.5 Å component of N IV] is of marginal significance. The FWHM was 0.19 Å for N III] and 0.18 Å for the C III] lines. Since the resolution is 0.16–0.20 Å, all lines are thus unresolved and we find an upper limit of $\sim$31 km s^{-1} for the velocity broadening along the line of sight (FWHM). For the later analysis it is also of interest to compare the total fluxes in the lines with the low-resolution observations. In the high-resolution spectra the position of the continuum is better defined and provides a valuable check on the effect of continuum level, especially for the C III] line. Correcting for the reddening, we obtain for the C III] line a flux 6.3×10^{-13} ergs cm^{-2} s^{-1}, and for the N III] line 9.3×10^{-13} ergs cm^{-2} s^{-1}. The corresponding values from the November 13 low-resolution observation for the same lines were 4.5×10^{-13} and 15.7×10^{-13} ergs cm^{-2} s^{-1}, respectively (Table 2). Since the errors in the high-resolution fluxes amount to $\sim$50%, these values are consistent and show that the flux of the C III] line as measured in the low resolution is not severely affected by the supernova background continuum.

It is also worth while to comment on the evolution of the intrinsic supernova continuum during this period. Virtually absent during March to May, the continuum increased steadily above $\sim$1700 Å and between $\sim$1300–1550 Å, until 1988 January. After this, however, the continuum slowly decreased. This can be seen clearly in Figure 2, where the background from the B stars has been subtracted. At the same time a wide absorption feature with an absorption minimum at $\sim$1878 Å has developed. The width of this feature indicates an expansion velocity of $\sim$3100 km s^{-1}, comparable to the expansion velocity of the IR Fe II 17.93 μm line (Moseley *et al.* 1988). It may thus be due to freshly synthesized material. There are also a number of other less prominent features in this region. As discussed in Fransson *et al.* (1987) and Lucy (1987), the continuum is likely to be a complicated result of many overlapping resonance lines, redshifting the photons in each scattering. The radiation thus escapes where the absorption is least, and does not provide much information about where it is created. It is, however, interesting that the wide feature between $\sim$1300 and 1550 Å may be an indication of emission in the O I resonance lines at 1300 and 1356 Å. These are both expected to be strong at late stages as a result of emission from the core and envelope (Fransson 1987). The increase in this region also occurs at the same time as the optical [O I] $\lambda\lambda$6300–6364 lines become strong (Danziger *et al.* 1988).

III. PHYSICAL PROPERTIES OF THE EMISSION-LINE REGION

a) Density and Temperature

In this section we apply a nebular analysis to the lines in Table 2 to determine the relative abundances and physical conditions of the emission-line region.

Although not observed, the absence of N IV λ1718 can provide a constraint on the temperature. Since N IV λ1718 mainly arises as a result of dielectronic recombination of N V, and N V λ1240 due to collisional excitation, this line ratio can be used to obtain a lower limit to the electron temperature in the N V zone. Using the recombination rate by Nussbaumer and Storey (1984), collision strength in Mendoza (1983), and adopting F(N IV λ1718)/F(N V λ1240) < 0.2, we find that the temperature must be higher than $\sim$12,000 K. A maximum temperature is obtained from the upper limit of the velocity dispersion of the He II line, corresponding to $\sim 9 \times 10^4$ K. Recently, observations of narrow [O III] forbidden optical lines have been reported by Wampler and Richichi (1988). It is most likely that these come from the same gas as the UV emission lines. With our $E(B-V) = 0.20$ and for a density of 10^4 cm^{-3}, the ratio of the 4959 + 5007 and 4363 Å lines corresponds to a temperature of $\sim$50,000 K for this gas, which at the moment is the only direct determination. From the absolute line strengths of these lines an independent check on the total reddening along the line of sight can be made using O III] λ1664. At the same epoch as the optical observations ($\sim$day 300), we find a flux of $\sim 5.0 \times 10^{-13}$ ergs cm^{-2} s^{-1} for the 1664 Å line. The total flux of the 4959 + 5007 Å lines was $\sim 8.3 \times 10^{-13}$ ergs cm^{-2} s^{-1} [using $E(B-V) = 0.20$], so F(1664)/F(4959 + 5007) $\sim$ 0.61. At 5.0×10^4 K the expected value is 0.77. Considering the uncertainties in the fluxes, this shows that our adopted reddening is consistent with these observations.

The relative strengths of the multiplet components of the C III], N III], and N IV] intercombination lines are highly useful as density diagnostics. Since all these lines are collisionally de-excited above $\sim 10^9$ cm^{-3}, the density must be less than this value. Our high-resolution observations of the C III] lines give a ratio of F(1906.7)/F(1908.7) $\sim$ 1.0. The calculations by Nussbaumer and Schild (1979) show that this implies that the electron density must be less than $\sim 3 \times 10^4$ cm^{-3}, for a temperature less than $\sim$50,000 K. For the N III] line we find that F(1749.7):F(1752.2):F(1754.0) $\sim$ 1:0.5:0.3, with a considerable uncertainty. The calculations by Czyzac, Keyes, and Aller (1986) show that below 10^2 cm^{-3} these ratios are 1:1.5:0.6, while above $\sim 10^4$ cm^{-3} they are 1:0.6:0.2. The N III] lines thus indicate that the density is larger than $\sim 1 \times 10^4$ cm^{-3}, so a consistent density is (1–3) $\times$ 10^4 cm^{-1}. The electron density can also be obtained from the ratio of the components of the N IV] $\lambda\lambda$1483.3–1486.5 multiplet. For densities higher than $\sim 10^4$ cm^{-3} the 1486.5 Å component dominates, whereas at lower densities the ratio of the 1483.3 and 1486.5 Å lines approaches 5/3 (Nussbaumer and Schild 1981). Unfortunately, the quality of the high-resolution data does not permit a diagnosis based on these observations. We have, however, measured the wavelength of the N IV] line for several dates in the low-resolution data, and find a peak wavelength of 1483.65 $\pm$ 1.15 Å. For the absolute wavelength calibration we have used the wavelengths of the strongest interstellar lines. Since the expected peak wavelength in the low-density limit is 1484.5 Å, the observed wavelength implies a density of less than $\sim 5 \times 10^4$ cm^{-3} in the region where N IV is present (Cassatella 1987), consistent with the high-resolution observations. In principle, the same procedure could be used for N III] $\lambda\lambda$1746.8–1754.0. For the N III] lines the mean wavelength, 1751 Å, does not, however, shift by more than $\sim$0.4 Å between the high- and low-density limits.

b) Abundances

From photoionization models of nebulae (e.g., Nussbaumer and Schild 1981), it is found that N III and C III occurs in the

same volume, as do N IV and C IV, whereas O III is present in both these zones. He III and N V are expected to be dominant in a more highly ionized region. Thus, lines of corresponding ionization stages of carbon and nitrogen arises in the same region. This is also found to be a reasonable approximation under most conditions in time-dependent calculations of the circumstellar ionization structure of SN 1987A (Lundqvist and Fransson 1987, 1988*b*). From the relative strengths in Table 2 we can therefore estimate the ratios of the abundances of these ions. Since the electron density is much less than 10^9 cm^{-3}, collisional de-excitation can be neglected. The line ratios are then a function only of the atomic parameters, the ionic abundances, and the temperature. The collision strengths are taken from the compilation by Mendoza (1983). We have adopted a value of 50,000 K for the temperature, typical of that found in photoionization models, and consistent with the optical and UV O III lines. Due to the weakness of the lines during the first months, we have used only the well-exposed spectra after July 20 for the abundance analysis. As a mean after this data we obtain the following ionic ratios: N(N III)/N(C III) = 7.79, N(N III)/N(O III) = 1.23, N(N IV)/N(N III) = 0.34, and N(N V)/N(N IV) = 0.74. Since the excitation energies are similar, these values depend only weakly on the adopted temperature. A temperature of 10^5 K would, for example, only decrease the N(N III)/N(C III) ratio to 7.29, while a temperature of 20,000 K would give 9.57. Instead, the main uncertainty in the N/C ratio comes from the flux of C III] λ1909. There is also some tendency for the early measurements (earlier than $\sim$300 days) to give a slightly higher N III]/C III] ratio than the more recent ones [N(N III)/N(C III) $\sim$ 9, compared with $\sim$6]. This may be an effect of the weakness of the C III] line, which has a larger scatter in the early measurements.

From the photoionization models we expect the N(N III)/N(N) and N(C III)/N(C) ratios to be approximately equal, and thus N(N III)/N(C III) $\sim$ N(N)/N(C). O III may, on the other hand, coexist together with both N III and N IV, and for the nitrogen-to-oxygen ratio we instead take N(N)/N(O) $\sim$ [N(N III) + N(N IV)]/N(O III). Thus, we find N(N)/N(C) = 7.79 and N(N)/N(O) = 1.60. The standard deviations in these values during the discussed period were σ = 2.4 and σ = 0.71, respectively.

The N/He ratio can in principle be obtained from the N V line and He II λ1640. This, however, depends sensitively on the assumed temperature and ionization structure. Using the most reliable observations, we find F(N V λ1240)/F(He II λ1640) $\sim$ 3.3, and thus N(N V)/N(He III) $\sim 5.2 \times 10^{-6} e^{11.6/t}$, where $t = T_e/10^4$ K. Using a temperature of 50,000 K, we find N(N V)/N(He III) $\sim 5.3 \times 10^{-5}$. The relation between N(N V)/N(He III) and N(N)/N(He) is, however, highly model-dependent. The photoionization models by Nussbaumer and Schild (1981) give N(N)/N(He) $\sim$ 2N(N V)/N(He III). On the other hand, models by Lundqvist and Fransson (1988*b*) give initially N(N)/N(He) $\sim$ 3N(N V)/N(He III), but later this ratio increases by a large factor because of the larger recombination rate of N V compared with He III. In view of this uncertainty and the temperature sensitivity, it is hard to conclude anything about the N/He ratio.

As a check on the systematic errors in this type of analysis, we have repeated the procedure on the *model* calculations of Nussbaumer and Schild (1981). We found that the N/C ratio was underestimated by $\sim$30%, whereas the N/O ratio was overestimated by $\sim$29%. To eliminate this uncertainty, more detailed model calculations are necessary. The error in the abundance estimate is, however, likely to be dominated by observational errors in the line strengths, especially the C III] λ1909 line (§ II). A lower limit to the N/C ratio can be obtained if we assume that there is *no* continuum contribution from the supernova for the C III] line, and that *only* the emission above the continuum is due to the N III] line. In this way we obtain a value of F(N III])/F(C III]) = 0.7 on the average October–November spectrum, resulting in a lower bound of N/C = 2.2 at 50,000 K. This is obviously a rather unrealistically extreme situation, especially in view of the agreement in the line fluxes between the high-resolution and the low-resolution observations. From the variance in the N III/C III ratio and the systematic errors in the continuum level and in the ionization model, we estimate a realistic error to be $\pm$4 in the N/C ratio. It is worth pointing out that a normal cosmic ratio of N/C $\sim \frac{1}{4}$ would give N III] $\lambda\lambda$1747–1754/C III] $\lambda\lambda$1907–1909 $\sim$ 0.06! For the O III] line the continuum is less of a problem, and most of the error in the N/O ratio is due to the weakness of the O III] line and the uncertainty in the ionization model. With the standard deviation above and the error in the ionization model we estimate an uncertainty of $\pm$0.8 in the N/O ratio. Summarizing, we thus obtain

$$N(\mathrm{N})/N(\mathrm{C}) = 7.8 \pm 4, \quad N(\mathrm{N})/N(\mathrm{O}) = 1.6 \pm 0.8 .$$

In terms of solar abundances (Cameron 1982), they become [N]/[C] = 37 $\pm$ 18 and [N]/[O] = 12 $\pm$ 6.

An estimate of the total emitting mass can be obtained from He II λ1640, assuming that recombination dominates. On day 300 after the explosion the luminosity of this line was $\sim 1.7 \times 10^{35}$ ergs s^{-1}. Using the effective recombination rate from Seaton (1978), we find an emitting mass of

$$5.8 \times 10^{-3} t^{0.84} \left(\frac{n_e}{10^4 \text{ cm}^{-3}} \right)^{-1} \left[\frac{N(\mathrm{He})}{N(\mathrm{He\ III})} \right] \left[1 + \frac{N(\mathrm{H})}{4N(\mathrm{He})} \right] M_\odot .$$

As a rough estimate we take N(He III)/N(He) $\sim$ 1 as found in ionization models. Thus, using $T \sim$ 50,000 K, N(He)/N(H) $\sim$ 0.2, and $n_e \sim 10^4$ cm^{-3}, we find an emitting mass of $\sim 0.1 (n_e/10^4 \text{ cm}^{-3})^{-1} M_\odot$. The thickness is then $\sim 1.2 \times 10^{15} (n_e/10^4 \text{ cm}^{-3})^{-1} (R_s/10^{18} \text{ cm})^{-2}$. Here R_s is the radius of the shell from the supernova. We stress, however, that because of the uncertainty in the density and in the ionization, these should only be considered as a rough estimate. If cooling and recombination are rapid, only a small fraction of the gas contributes to the emission.

IV. ORIGIN OF THE EMISSION LINES

There are several possible sources for the observed emission lines: They could come either from processed material in the He/O core inside the supernova, from circumstellar gas lost by the progenitor of the supernova, or from the interstellar medium. There are several arguments against the core interpretation. With a core expansion velocity of $\sim$2000 km s^{-1} and a core mass of $\sim 4 M_\odot$, the atomic density in the core is expected to be $\sim 1.5 \times 10^{10}$ cm^{-3} at 100 days. The electron density would be several times larger than this value, for the observed ionization state. This is even larger than the density at which collisional de-excitation of the N III], N IV], and C III] lines sets in, and is in conflict with the derived density from the N IV] line ratios. The nitrogen lines would also be expected to have velocities larger than 1000 km s^{-1} if they came from the supernova ejecta. Emission from the core region is expected mainly as lines of oxygen, e.g., O III] λ1664 (Fransson 1987),

rather than nitrogen. It is also difficult to understand how the emission could escape from the core without being scattered by the many resonance lines from the fast-moving envelope. The narrow line widths from the high-dispersion observations rule out the core scenario effectively. An origin in the general interstellar medium around the supernova also meets considerable difficulties, mainly because of the anomalous N/C ratio, the large density, and high ionization.

If the lines come from circumstellar gas expelled from the supernova progenitor, the deduced properties are easier to understand. The density is expected to be low, with the exact value dependent on both the mass-loss history of the progenitor and the precise location of the UV-emitting gas. In this context it is interesting that the early radio observations of SN 1987A (Turtle *et al.* 1987) provide strong evidence for circumstellar gas up to at least $\sim 2 \times 10^{16}$ cm from the supernova (Chevalier and Fransson 1987). This is likely to be due to the low-density, fast (~ 550 km s^{-1}) wind from the blue supergiant phase. The density of this component is, however, too low, $\sim 0.2(r/10^{18}\ \mathrm{cm})^{-2}$ cm^{-3}, to be responsible for the emission. Many evolutionary models, however, predict that the blue supergiant phase of Sanduleak $-69°202$ was preceded by a phase as a red supergiant (e.g., Maeder 1987; Woosley, Pinto, and Ensman 1988; Saio, Nomoto, and Kato 1988). The time scale between these stages is uncertain, but is probably in the range 10^3–10^5 yr. The density of the undisturbed red supergiant wind outside the interaction region is only $\sim 20(\dot{M}/10^{-5}\ M_\odot\ \mathrm{yr}^{-1})\,(r/10^{18}\ \mathrm{cm})^{-2}$ cm^{-3} for a wind velocity of 10 km s^{-1} and mass loss rate $\dot{M}$. It is thus unlikely as the origin of the observed emission. The interaction region between the fast wind in the blue stage (velocity ~ 550 km s^{-1}) and the slow wind from the earlier red stage (velocity ~ 10 km s^{-1}) is, however, expected to give rise to a region of dense shocked gas as the fast wind sweeps up the slow red supergiant wind. There will then be one shock propagating into the slow outer wind and one propagating into the fast wind. The two regions of shocked gas will be separated by a contact discontinuity. The dynamics of this region have been discussed by Chevalier and Imamura (1983), who find a similarity solution describing the structure. As discussed by Chevalier (1987), the outer of these shocks will be radiative, and the density enhancement compared with the red supergiant wind will be ~ 50–1000. Chevalier estimates that a likely density in this shell is $\sim 10^3$–10^4 cm^{-3}. The exact density distribution, however, depends on the importance of instabilities, which may break up the shell into filaments. The estimate of the shell thickness in § III is consistent with that expected from a cooling shell. The velocity of the shell is approximately given by $V_s \propto V_b^{2/3} V_r^{1/3} (\dot{M}_b/\dot{M}_r)^{1/3}$, where V_b and $\dot{M}_b$ are the velocity and mass-loss rate of the blue supergiant wind, and V_r and $\dot{M}_r$ the same for the red wind. The ratio of the mass-loss rates in the red and blue stages is uncertain, but is likely to be in the range 1–50. For typical values of $V_b = 550$ km s^{-1} and $V_r = 10$ km s^{-1} one finds $V_s \sim 130\ (\dot{M}_b/\dot{M}_r)^{1/3}$ km s^{-1}. The radius of this shell will be determined by the lifetime in the final blue supergiant stage and $\sim (1.5$–$4) \times 10^{18}$ cm, depending on $\dot{M}_b/\dot{M}_r$ (Chevalier 1987).

Several Wolf-Rayet stars possess thin shells, likely to be due to stellar wind interaction or ejection. Solf and Carsenty (1982) find that the WN8 star 109 BAC is surrounded by an expanding shell of radius ~ 0.93 pc and thickness less than 0.05 pc, and an expansion velocity of 42 km s^{-1}. The electron density is $\sim 10^3$ cm^{-3}, and the mass is estimated to be $\sim 0.8\ M_\odot$. Soft and Carsenty argue that the shell is the result of the interaction of the wind, or an ejected shell from the Wolf-Rayet star, with gas previously lost by the star. Although Sanduleak $-69°202$ was not a Wolf-Rayet star, the situation closely resembles this case. There is also substantial evidence for extended circumstellar gas around several late supergiants, such as α Ori (Mauron *et al.* 1984), μ Cep (Mauron *et al.* 1986), and the Cepheid RS Pup (Havlen 1972). The radii of these shells are 10^{17}–10^{18} cm, and the total mass may be several solar masses. These observations indicate more episodic mass loss, creating discrete, multiple shells, which may be important in the interpretation of the history of the SN 1987A progenitor, as well as future observations. Therefore, we find that the most likely explanation for the gas is either the gas in the interaction region between the fast blue supergiant wind and the slow red supergiant wind, or, perhaps less likely, gas resulting from an ejected shell.

The energy source for the emission may be either the radiation from the expanding supernova shock wave, X-rays from the interior of the supernova, or the early EUV burst from supernova breakout. An obvious requirement is that the source must supply the necessary luminosity on a time scale of $\sim 10^7$ s. We have integrated the total line flux in the UV and find that the received flux corresponds to an energy of $\sim 5.7 \times 10^{43}$ ergs from the time of the explosion to 1988 April 14. In addition, there may be strong lines below 1200 Å as well as in the optical, drowned by the radiation from the supernova. The minimum total energy necessary is thus at least $\sim 10^{44}$ ergs. Unless the density of the blue supergiant wind decreases more slowly than r^{-2}, the luminosity from the interaction of the shock and circumstellar gas is, however, only $\sim 10^{35}$–10^{36} ergs s^{-1} (Chevalier and Fransson 1987), too small for the emission lines. SN 1987A has been observed in X-rays by Ginga (Dotani *et al.* 1987) and by MIR (Sunyaev *et al.* 1987). The soft component seen by Ginga below ~ 10 keV had a luminosity of $\sim 2 \times 10^{37}$ ergs s^{-1} in September, and could in principle provide the necessary energy. However, with our estimate of the mass in the shell, the column density is only $\sim 1 \times 10^{19}(R_s/10^{18}\ \mathrm{cm})^{-2}$ cm^2. Although this estimate is rough, it shows that the column density is too small to absorb any X-rays even at 1 keV. The emission lines also appeared in May, and there is no obvious correlation in strength between the X-rays and the UV-emission lines.

We think that the early EUV burst is the most likely source of energy. Hydrodynamical models show that during the first hours an energy of $\sim 10^{46}$–10^{47} ergs with a radiation temperature of $\sim (3$–$5) \times 10^5$ K was emitted from SN 1987A (Shigeyama, Nomoto, and Hashimoto 1988; Woosley 1988). Calculations show that this radiation ionizes all ions with ionization potentials less than ~ 100 eV (e.g., up to N VI), as well as increases the temperature (Lundqvist and Fransson 1987, 1988*b*). However, since the recombination time from, e.g., N VI to N V is $525(n_e/10^4\ \mathrm{cm}^{-3})^{-1}$ days and from N V to N IV is $\sim 34\ (n_e/10^4\ \mathrm{cm}^{-3})^{-1}$ days at 10^5 K, the gas will have time to recombine into the observed stages. If the density is much lower than 10^4 cm^{-3}, the observed ionization state depends critically on the spectral shape of the burst, since it is "frozen in" to the gas. The density necessary for recombination to be important is consistent with that derived in § III. At the high temperatures encountered in the gas, dielectronic recombination dominates for N III–N V.

The time evolution is governed by a combination of recombination and light travel time effects. For a thin shell of radius R_s, larger than ct, the volume of the shell visible to us increases

as $\sim 2\pi R_s ct\Delta R$, where c is the velocity of light and ΔR the thickness of the shell. A finite thickness does not change this dependence appreciably. We can now separate two limiting cases: If the recombination time and cooling time are long compared with the light travel time, so that the temperature and degree of ionization in the shell are constant, the received flux will be just proportional to the volume, $\sim 2\pi R_s ct\Delta R$, and the luminosity will increase linearly with time. On the other hand, if these time scales are shorter than $\sim R_s/c$, the evolution will proceed on the recombination time scale. Superposed on this, there will be a long-term evolution determined by the light travel time. In this latter case the ionization state and thus the line ratios will vary with time, while in the former the variations will be smoothed out over a longer period. This should be compared with the observed variation in Figure 3. The most apparent evolution can be seen for the N III] and N V lines. After ~ 100 days the time evolution can be fairly well approximated with a straight line, indicating that the light echo effect is important for the time evolution. This rise is expected to stop when the whole region is visible to us, and then stay constant until recombination sets in. We do not, however, think that this alone can explain the evolution. First, the turn-on of the flux does not occur until ~ 70 days after the explosion. While the fluxes of the first few points are rather uncertain, and small fluxes may elude detection, also the slope of the line is too steep to pass through the origin, indicating that both recombination and light echo effects are important. The fact that both the N III]/N IV] ratio and the N V/N IV] ratio clearly change with time also shows that the state of ionization changes (Fig. 3). Thus, recombination is likely to be important, implying that the density exceeds $\sim 10^4$ cm^{-3}, in line with the density derived from the N III] and C III] lines. The C III] line resembles the N III] line, as expected, while the scatter in the O III] flux makes any conclusions from this uncertain. Although a more detailed calculation is clearly necessary (Lundqvist and Fransson 1988*b*), the qualitative time evolution is consistent with a picture in which both light travel time and recombination play a role.

In the simple case of a spherical shell, and if recombination is slow, the radius of the shell is given by $R_s \sim ct_c/2$. Here t_c is the time when the whole shell is visible to us, and the flux becomes constant with time. A constant phase is, however, also expected if the recombination time scale is short. Up to 1988 April only a marginal flattening of the light curve can be seen in N III], N V, and C III]. A time scale of 400 days corresponds to a minimum shell radius of $\sim 5 \times 10^{17}$ cm. Firmer conclusions will be possible from the coming evolution, especially the decay of the flux, since this directly reflects the recombination time scales. The visible radius of the shell is expected to be

$$\sim 1.8(R_s/10^{18}\ \mathrm{cm})^{1/2}(t/400\ \mathrm{days})^{1/2}(1 - ct/2R_s)^{1/2}\ \mathrm{arcsec}\ ,$$

increasing until $t = R_s/c \sim (R_s/10^{18}$ cm) yr. From an examination of the N V line from 1988 April we find an upper limit of $\sim 2''$ for the diameter, assuming a uniformly emitting disk. This corresponds to a maximum distance of $\sim 8 \times 10^{17}$ cm from the supernova to the shell. The optical observations of [O III] λ5007 give a FWHM extent of $\sim 2''$, corresponding to a distance of $\sim 10^{18}$ cm, comparable to our limit (Wampler and Richichi 1988). The observed expansion velocity is given by μV_s, where μ is the cosine of the angle between a point on the shell and the line of sight. In the case of a short recombination time, only a thin region with $\mu = 1 - ct/R_s$ will contribute, and the peak velocity of the line will thus decrease with time and finally become *redshifted* with a peak wavelength $\lambda_0(1 + V_s/c)$. In the case of a long recombination time the width of the line will increase in a similar manner. Since V_s is likely to be in the range 40–150 km s^{-1} for $\dot{M}_r/\dot{M}_b$ in the range 1–50, and the resolution in the high-dispersion mode is ~ 30 km s^{-1}, this wavelength shift is likely to be observable with future high-resolution observations. Similar conclusions have been reached by Chevalier (1988). We point out, however, that at present there is no indication that the geometry really is that of a shell. It could be, e.g., a plane sheet or a cloud with a transverse dimension

$$ct(2R_s/ct - 1)^{1/2} \approx (2R_s ct)^{1/2}\ .$$

The absence of a shift in wavelength would be an indication of this geometry.

A future confirmation of variability of the lines could give information about a possible nonuniform structure of the circumstellar gas. As the region observable to us grows, new filaments become visible, and if the recombination time is short, this will be seen as fluctuations in the line fluxes. We also remark that the presence of dense circumstellar gas may be important for the interaction of the supernova ejecta in the future, leading to increased X-ray emission (Itoh *et al.* 1987). Since the maximum expansion velocity of the supernova was $\sim 0.1c$, this will take place after $\sim 10(R_s/10^{18}$ cm) yr.

V. NATURE OF THE PROGENITOR

The most important result in this paper is the large value of the N/C ratio implied by the emission lines. A similar result was obtained for the "normal" Type II supernova SN 1979C, where N/C was 8 ± 3 (Fransson *et al.* 1984). There it was argued that this was a result of the CNO burning in combination with strong mass loss and envelope mixing. Since mass loss was probably even more important for SN 1987A, we think that this is a likely explanation also in this case. Maeder (1987) has calculated the evolution of a 20 $M_\odot$ ZAMS star, with different mass-loss rates and convective mixing. It is found that after passing from the red supergiant stage, when the total mass is only $\sim 12.6\ M_\odot$, the surface value of N/C increases from ~ 0.2 to ~ 100, while N/O increases from $\sim \frac{1}{9}$ to ~ 2.5. At the same time there is a steady increase in the surface He/H ratio. These changes are typical of material which has undergone CNO processing, with the CN cycle operating close to equilibrium, while the ON cycle, converting oxygen into nitrogen, has not reached its equilibrium value. At the time of the explosion the total mass in Maeder's model is constrained to be ~ 8.6–$10\ M_\odot$ in order for the star to explode as a blue supergiant. Even though the detailed results are sensitive to the imput physics, in particular to the adopted mass-loss rates and the convective mixing efficiency, we think that evolution through extensive mass loss qualitatively may explain the observations. The total mass lost may thus be as high as $\sim 10\ M_\odot$. Also, from analysis of the light curve of SN 1987A, it has been argued that several solar masses of the envelope had been lost by the progenitor (Shigeyama, Nomoto, and Hashimoto 1988; Woosley, Pinto, and Ensman 1988). These authors, however, find that a minimum envelope mass of $\sim 3\ M_\odot$ is needed to avoid He core expansion velocities that are too large. This is considerably more than the value found by Maeder in his model. Saio, Nomoto, and Kato (1988) have recently discussed models with moderate mass loss, fulfilling this criterion. In this scenario the blue-red-blue evolution is critical to the helium abundance in the envelope. In order to

obtain the needed helium enrichment at the surface, complete mixing of the hydrogen envelope is necessary, and possibly even a dredge-up of some of the helium shell. To reproduce the observed nitrogen enrichment, Saio *et al.* then find that the mass of the mixed hydrogen envelope is constrained to be 7.5–11 $M_\odot$ (total mass 13.5–17 $M_\odot$ at the time of the explosion). Too small a hydrogen mass, less than $\sim$1–2 $M_\odot$, may also conflict with the mass needed to explain the optical spectrum. Models of the envelope by Höflich (1987) and Eastman and Kirshner (1988) are important in determining this mass. A determination of the He/H ratio in the envelope of SN 1987A is obviously of great interest.

As already mentioned, there is other independent evidence for mass loss of the SN 1987A progenitor. The radio observations of SN 1987A imply a mass-loss rate of $\sim 8.6 \times 10^{-6}\ M_\odot\ \mathrm{yr}^{-1}$, for a wind velocity of 550 km s^{-1} (Chevalier and Fransson 1987), meaning that an appreciable mass may have been lost on a time scale of $\sim 10^5$ yr. In Maeder's models most of the mass loss, however, occurs in the red supergiant phase. From our previous discussion we think that the emitting gas is likely to be the result of the red supergiant wind shocked by the blue wind. Therefore, these observations provide evidence for a previous phase as a red supergiant.

Large N/C ratios have also been observed in other related objects. The quasi-stationary flocculi in Cas A display an overabundance of nitrogen by a factor of 3–7, compared with solar (Chevalier and Kirshner 1978). This has been explained by Lamb (1978) as a result of CNO burning in combination with mass loss. The low velocities indicate a circumstellar origin, presumably due to previous mass loss. Also, the recently found fast-moving flocculi in Cas A show strong evidence for CNO processing (Fesen, Becker, and Blair 1987). Because of their very high velocities, Fesen *et al.* interpret this as CNO-processed material from the photospheric layers of the Cas A progenitor. A similar situation is present for the Pup A supernova remnant, which also displays strongly nitrogen-enriched filaments (Baade and Minkowski 1954; Dopita, Mathewson, and Ford 1977). With regard to potential supernova progenitors, some condensations around the very massive (presupernova?) star η Car have a UV spectrum similar to that of SN 1987A, indicating CNO burning and He enrichment. From their UV observations Davidson *et al.* (1986) derive a N/C ratio of $\sim$50, as well as an increased He fraction. Several Wolf-Rayet stars have nitrogen-rich nebulae surrounding the star (Kwitter 1984). Also, a number of blue supergiants in the LMC and SMC show high N/C and N/O ratios, as well as He enhancement (Kudritzki 1987). The same was shown to be the case also for a number of G and K supergiants in our Galaxy by Luck and Lambert (1981). The enhancements for these, however, are only a factor of $\sim$3–4 times solar.

Therefore, from this evidence it is clear that mass loss is a very important factor in the evolution of the massive stars leading to core-collapse supernovae. We already know that "normal" Type II progenitors, where the progenitor is likely to have been a red supergiant, have large mass-loss rates. For SN 1979C and SN 1980K radio observations imply mass-loss rates of $\sim 1.2 \times 10^{-4}\ M_\odot\ \mathrm{yr}^{-1}$ and $3 \times 10^{-5}\ M_\odot\ \mathrm{yr}^{-1}$, for a wind velocity of 10 km s^{-1}, respectively (Lundqvist and Fransson 1988*a*). One may then speculate that stars of 10–15 $M_\odot$ suffer little mass loss, and explode as red supergiants ("normal" Type II's), while heavier stars, like Sanduleak $-69°202$, suffer more mass loss and move toward the blue before exploding. The fact that the observed mass-loss rates are higher for "normal" Type II progenitors is not in conflict with this, since the mass-loss rates reflect only their position in the H-R diagram and not the total mass lost. The most extreme examples of this type may be the Type Ib supernovae, where the progenitor is likely to have lost all its hydrogen envelope. As several calculations have shown, the evolutionary track is, however, a complicated function of mass loss, metallicity, helium abundance, and the treatment of the convection.

VI. CONCLUSIONS

The identification of Sanduleak $-69°202$ with the progenitor of SN 1987A has given us a unique test of the theories for the final moments of stellar evolution. The UV observations reported in this paper provide us with a further probe of the past history of the progenitor. In particular, we have found strong evidence that the progenitor had already lost a large fraction of its mass before the explosion. Together with other observational evidence, the nitrogen enrichment is a strong constraint on the structure of the envelope of the progenitor. If our interpretation of the source of excitation of the emission lines is correct, these observations also give us a chance to study the outbreak of the shock wave only a few hours after the explosion, before the discovery of SN 1987A.

The observations on which this work is based would not have been possible without the generous cooperation of the many *IUE* observers and the *IUE* Observatory staff. We are deeply grateful for their patience and understanding. We are also grateful for discussions of this work with many colleagues, especially Roger Chevalier, Peter Lundqvist, and Joe Wampler. This work has been supported by National Aeronautics and Space Administration grants NAG5-841, NAG5-645, NAG5-87, National Science Foundation grant AST85-16537, and the Swedish Board of Space Activities.

REFERENCES

Baade, W., and Minkowski, R. 1954, *Ap. J.*, **119**, 206.
Blades, J. C., Wheatley, J., Panagia, N., Grewing, M., Pettini, M., and Wamsteker, W. 1988, *Ap. J.*, **334**, 000.
Cameron, A. G. W. 1982, in *Essays in Nuclear Astrophysics*, ed. C. A. Barnes, D. D. Clayton, and D. N. Schramm (Cambridge: Cambridge University Press), p. 23.
Cassatella, A. 1987, in *Proc. ESO Workshop on the SN 1987A*, ed. I. J. Danziger (Munich: ESO), p. 101.
Cassatella, A., Barbero, J., and Benvenuti, P. 1985, *Astr. Ap.*, **144**, 335.
Cassatella, A., Fransson, C., Gilmozzi, R., Kirshner, R. P., Panagia, N., Sonneborn, G., and Wamsteker, W. 1988, in preparation.
Cassatella, A., Fransson, C., van Santvoort, J., Gry, C., Talavera, A., Wamsteker, W., and Panagia, N. 1987, *Astr. Ap.*, **177**, L29.
Chevalier, R. A. 1987, in *Proc. ESO Workshop on the SN 1987A*, ed. I. J. Danziger (Munich: ESO), p. 481.
———. 1988, *Nature*, **332**, 514.
Chevalier, R. A., and Fransson, C. 1987, *Nature*, **328**, 44.
Chevalier, R. A., and Imamura, J. N. 1983, *Ap. J.*, **270**, 554.
Chevalier, R. A., and Kirshner, R. P. 1978, *Ap. J.*, **219**, 931.
Czyzak, S. J., Keyes, C. D., and Aller, L. H. 1986, *Ap. J. (Suppl.)*, **61**, 159.
Danziger, I. J., Bouchet, P., Fosbury, R. A. E., Gouiffes, C., Lucy, L. B., Moorwood, A. F. M., Oliva, E., and Rufener, F. 1988, in *Proc. Fourth George Mason Fall Workshop in Astrophysics, Supernova 1987A in the Large Magellanic Cloud*, in press.
Davidson, K., Dufour, R. J., Walborn, N. R., and Gull, T. R. 1986, *Ap. J.*, **305**, 867.

de Boer, K. S., Grewing, M., Richtler, T., Wamsteker, W., Gry, C., and Panagia, N. 1987, *Astr. Ap.*, **177**, L37.
Dotani, T., *et al.* 1987, *Nature*, **330**, 230.
Dopita, M. A., Mathewson, D. S., and Ford, V. L. 1977, *Ap. J.*, **214**, 179.
Dupree, A. K., Kirshner, R. P., Nassiopoulos, G. E., Raymond, J. C., and Sonneborn, G. 1987, *Ap. J.*, **320**, 597.
Eastman R., and Kirshner, R. P. 1988, in preparation.
Fesen, R. A., Becker, R. H., and Blair, W. P. 1987, *Ap. J.*, **313**, 378.
Fitzpatrick, K. C. 1986, *A.J.*, **92**, 1068.
Fransson, C. 1987, in *Proc. ESO Workshop on the SN 1987A*, ed. I. J. Danziger (Munich: ESO), p. 467.
Fransson, C., Benvenuti, P., Gordon, C., Hempe, K., Palumbo, G. G. C., Panagia, N., Reimers, D., and Wamsteker, W. 1984, *Astr. Ap.*, **132**, 1.
Fransson, C., Grewing, M., Cassatella, A., Panagia, N., and Wamsteker, W. 1987, *Astr. Ap.*, **177**, L33.
Gilmozzi, R., *et al.* 1987, *Nature*, **328**, 318.
Havlen, R. J. 1972, *Astr. Ap.*, **16**, 252.
Höflich, P. 1987, in *Proc. ESO Workshop on the SN 1987A*, ed. I. J. Danziger (Munich: ESO), p. 449.
Itoh, H., Hayakawa, S., Masai, K., and Nomoto, K. 1987, *Pub. Astr. Soc. Japan*, **39**, 529.
Kirshner, R. P. 1988, in *IAU Colloquium 108, Atmospheric Diagnostics of Stellar Evolution: Chemical Peculiarity, Mass Loss, and Explosion*, ed. K. Nomoto (Berlin: Springer), p. 252.
Kirshner, R. P., Sonneborn, G., Cassatella, A., Gilmozzi, R., Panagia, N., and Wamsteker, W. 1987*b*, *IAU Circ.*, No. 4435.
Kirshner, R. P., Sonneborn, G., Crenshaw, D. M., and Nassiopoulos, G. E. 1987*a*, *Ap. J.*, **320**, 602.
Kudritzki, R. 1987, in *Proc. ESO Workshop on the SN 1987A*, ed. I. J. Danziger (Munich: ESO), p. 39.
Kwitter, K. B. 1984, *Ap. J.*, **287**, 840.
Lamb, S. 1978, *Ap. J.*, **220**, 186.
Luck, R. E., and Lambert, D. L. 1981, *Ap. J.*, **245**, 1018.
Lucy, L. B. 1987, *Astr. Ap.*, **182**, L31.
Lundqvist, P., and Fransson, C. 1987, in *Proc. ESO Workshop on the SN 1987A*, ed. J. Danziger (Munich: ESO), p. 495.
———. 1988*a*, *Astr. Ap.*, **192**, 221.
———. 1988*b*, in preparation.
Maeder, A. 1987, in *Proc. ESO Workshop on the SN 1987A*, ed. J. Danziger (Munich: ESO), p. 251.
Mauron, N., Cailloux, M., Tilloles, P., and Le Fevre, O. 1986, *Astr. Ap.*, **165**, L9.
Mauron, N., Fort, B., Querci, F., Dreux, M., Fauconnier, T., and Lamy, P. 1984, *Astr. Ap.*, **130**, 341.
Mendoza, C. 1983, in *IAU Symposium 103, Planetary Nebulae*, ed. D. R. Flower, (Dordrecht: Reidel), p. 143.
Moseley, H., Dwek, E., Glaccum, W., Graham, J., Loevensten, R., and Silverberg, R. 1988, *IAU Circ.*, No. 4576.
Nussbaumer, H., and Schild, H. 1979, *Astr. Ap.*, **75**, L17.
———. 1981, *Astr. Ap.*, **101**, 118.
Nussbaumer, H., and Storey, P. J. 1984, *Astr. Ap. Suppl.*, **56**, 293.
Panagia, N., Gilmozzi, R., Cassatella, A., Wamsteker, W., Kirshner, R. P., and Sonneborn, G. 1987*b*, *IAU Circ.*, No. 4514.
Panagia, N., Gilmozzi, R., Clavel, J., Barylak, M., Gonzalez Riesta, R., Lloyd, C., Sanz Fernandez de Córdoba, L., and Wamsteker, W. 1987*a*, *Astr. Ap.*, **177**, L25.
Saio, H., Nomoto, K., and Kato, M. 1988, *Nature*, **334**, 508.
Savage, B. D., and Mathis, J. S. 1979, *Ann. Rev. Astr. Ap.*, **17**, 73.
Seaton, M. J. 1978, *M.N.R.A.S.*, **185**, 5P.
Shigeyama, T., Nomoto, K., and Hashimoto, M. 1988, *Astr. Ap.*, **196**, 141.
Solf, J., and Carsenty, U. 1982, *Astr. Ap.*, **116**, 54.
Sonneborn, G., Altner, B., and Kirshner, R. P. 1987, *Ap. J. (Letters)*, **323**, L35.
Sunyaev, R., *et al.* 1987, *Nature*, **330**, 227.
Turtle, A. J., *et al.* 1987, *Nature*, **327**, 38.
Vidal-Madjar, A., Andreani, P., Cristiani, S., Ferlet, R., Lanz, T., and Vladilo, G. 1987, *Astr. Ap.*, **177**, L17.
Walborn, N. R., Lasker, B. M., Laidler, V. G., and Chu, Y.-H. 1987, *Ap. J. (Letters)*, **321**, L41.
Wampler, E. J., and Richichi, A. 1988, *Astr. Ap.*, submitted.
Wamsteker, W., Gilmozzi, R., Cassatella, A., and Panagia, N. 1987*b*, *IAU Circ.*, No. 4410.
Wamsteker, W., *et al.* 1987*a*, *Astr. Ap.*, **177**, L21.
Woosley, S. E. 1988, *Ap. J.*, **330**, 218.
Woosley, S. E., Pinto, P. A., and Ensman, L. 1988, *Ap. J.*, **324**, 466.

ANGELO CASSATELLA, ROBERTO GILMOZZI, and WILLEM WAMSTEKER: *IUE* Observatory, European Space Agency, P.O. Box 54065, Madrid, Spain

CLAES FRANSSON: Stockholm Observatory, S-13300 Saltsjöbaden, Sweden

ROBERT P. KIRSHNER: Harvard-Smithsonian Center for Astrophysics, 60 Garden Street, Cambridge, MA 02138

NINO PANAGIA: Space Telescope Science Institute, 3700 San Martin Drive, Baltimore, MD 21218

GEORGE SONNEBORN: *IUE* Observatory, Code 684.9/CSC, Goddard Space Flight Center, Greenbelt, MD 20771